Enhancing Achievable Information Rate via RMS-optimized Digital Pre-emphasis for Coherent Short Reach Applications

Wing Chau Ng, Qingyi Guo, Junho Chang, Chunpo Pan, Meng Qiu, Xuefeng Tang, Zhiping Jiang and Chuandong Li

Huawei Technologies Co., Ltd., Ottawa, ON K2K 3J1, Canada, wing.chau.ng@huawei.com

Abstract *We revisit the achievable information rate (AIR) due to the coupling between digital pre-emphasis and the bandwidth-limited channel under Tx constraints. We propose and experimentally verify, for the first time, a parameter-insensitive, RMS-optimized pre-emphasis filter for shaping high-frequency signal components to enhance the operational AIR.*

Introduction

As chromatic dispersion and four-wave mixing limit the reach of the intensity-modulation direct-detection (IM-DD) systems for the future 3.2T data center interconnects, coherent solutions would become necessary for unamplified links (UL) or even short reach (SR) starting from 2024 [1,2]. Hardware-wise, not only finite bandwidth (BW) and limited digital-to-analog converter (DAC) resolution, per-lane single-carrier (SC) coherent transceivers also suffer from limited transmitter (Tx) power [3-4], while the Tx power level directly affects the optical link loss budget for UL and SR [2,5]

Digital pre-emphasis (DPE) is usually employed to reduce both intersymbol interference (ISI) and receiver (Rx) DSP-enhanced noise, but the pre-emphasized waveforms may suffer from higher peak-to-average-power ratios (PAPRs). Their root-mean-square (RMS) or power needs to be "confined" to avoid excessive driver nonlinearity. This "power constraint" is also required to derive the theoretical channel capacity [6, (23)]. Recent works [5,7] restore signal's RMS for better performance by avoiding high-frequency components, but a mathematical interpretation of shaping the high-frequency pre-emphasized content is hitherto not available.

In practice, under the above Tx power constraint, a sharp S21 roll-off (channel itself) "couples" with the indispensable DPE, reappearing as a "new" physical channel with a reduced channel signal-to-noise ratio (SNR). This phenomenon can be revealed by observing the available optical signal-to-noise-ratio (OSNR) after the modulator or at the Rx side. Shaping input symbol distributions has been demonstrated to obtain slightly higher Tx signal powers [8,9], but is insufficient to maximize the achievable information rate (AIR) because the original channel law, $p_{\underline{y}|\underline{x}}$, has been changed by DPE to a "new" auxiliary channel $q_{\underline{y}|\underline{x}}$ [10, Ch. 4].

In this regard, we first revisit the AIR due to the coupling between the DPE and the BW-limited channel under Tx constraints. Next, various types of DPE are reviewed. Then, we propose, for the first time, a frequency-partitioned DPE filter optimization to enhance the operational AIR, by employing an RMS control to shape high-frequency signal components, which provides a self-contained interpretation based on the interplay between ISI, signal's RMS and the DAC's quantization noise suggested in [7].

Revisiting AIR due to the coupling between DPE and BW-limited channel

Fig. 1 shows the channel model of interest. The channel output is $y = c * h * x + c * n_q + n$ in time domain, denoted by lowercase letters, or $Y(f) = C(f)H(f)X(f) + C(f)N_Q + N(f)$ in frequency domain, denoted by uppercase letters. x is the channel input (QAM signals). h is the DPE filter. c is the channel (Tx response). n is the overall additive coloured noise. n_q is the uniformly distributed quantization noise, whose PSD, S_Q, is assumed flat [11]: $S_Q = \sigma_q^2 / B_e$, where B_e is the Tx-DSP BW, and $\sigma_q^2 = \langle |n_q|^2 \rangle = \left[\frac{(h*x)_{\max}}{2^{n_b - 1}}\right]^2 /12$, with n_b being the effective number of bits (ENoB). Statistical independence is assumed, i.e., $x \perp n_q \perp n$. For large ENOBs and $C(f) = 1$, the ideal per-polarization (per-symbol) AWGN channel capacity (bits/s/Hz) is

$$C_{\mathrm{AWGN}} = \log_2(1 + \langle |x|^2 \rangle / \langle |n|^2 \rangle). \quad (1)$$

Heuristically, the BW-limited channel, $C(f)$, limits the available in-band power throughput, and C_{AWGN} is lower-bounded by the BW-limited AWGN channel capacity (bits/s/Hz):

$$C_{\mathrm{ISI}} = \log_2(1 + \langle |c * x|^2 \rangle / \langle |n|^2 \rangle). \quad (2)$$

DPE could ideally bring C_{ISI} back to C_{AWGN} by

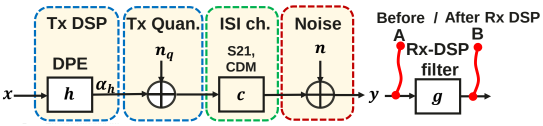

Fig. 1: Channel model. $\boldsymbol{h}$: Tx DPE filter, $\boldsymbol{c}$: ISI channel.

$H(f) = 1/C(f)$ with a perfect Tx. Due to the coupling between DPE and BW-limited C via Tx constraints, however, the "new" physical channel can be simplified to $y = c * \alpha_h(h * x) + n$, where α_h is a scaling factor in Tx-DSP required to adjust the RMS to avoid driver's nonlinearity: A sharper roll-off of C enhances the PAPR of $h * x,$ resulting in a smaller α_h, i.e., a reduced channel SNR. More generally, probabilistic shaping and a DPE filter, h, should be jointly designed to avoid small α_h, in order to attain the symbol-wise (SW) AIR,

$$\max_{p(\underline{x}),h}\left\{\sum_{\underline{x}} p_{\underline{x}} \int q_{\underline{y}|\underline{x}} \log_2\left(\frac{q_{\underline{y}|\underline{x}}}{\sum_{\underline{x}} p_{\underline{x}} q_{\underline{y}|\underline{x}}}\right) dy\right\} \le C_{\mathrm{ISI}} \le C_{\mathrm{AWGN}}, \tag{3}$$

and similarly for the bit-wise AIR as well [12], Ch. 4]. It is because the optimal h may not perfectly remove ISI, or a slightly high PAPR may also be allowed to obtain more power at the expense of driver's nonlinearity. Here, we only consider the linear operation of the driver.

Literature Review of DPE

The state-of-the-art DPE optimization can be classified into two types. The first type considers both Tx DPE and Rx DSP to maximize signal-to-noise ratio (SNR) or minimize the error or noise of Rx-DSP at location B in Fig. 1. Examples include Rx-zero-forcing (ZF) [13,14], and Rx-minimum mean square error (MMSE) [15]. For Rx-ZF with a known $C(f)$, refs. [13,14] separately claim that the optimal DPE filter shape should be $1/C(f)^{2/3}$, and $1/C(f)^{1/2}$, respectively. Several experimental works [7,15] rather adopted the n[th] root method: $H = 1/|C(f)|^{\beta}, 0 \le \beta \le 1$, where β is the "strength" of DPE not necessarily 2/3 nor 1/2, because Tx's RMS loss and quantization contribute to SNR degradation [7].

The second type considers only Tx DPE without Rx DSP, in an attempt to maximize the SNR before Rx DSP [11], at location A in Fig. 1. This could be justified by the "data processing inequality" that Rx DSP does not further increase the information content. Also, mitigating as much as ISI before the Rx reduces DSP enhanced noise. Ref. [11] proposed a Tx-MMSE approach to minimize ISI and n_q. To explain [11], let us define error, $e = y - x,$ at location A in Fig. 1. The peak value is proportional to the pre-emphasized signal power, i.e., $[(h * x)_{\max}]^2 = k\langle |h * x|^2\rangle = k\int |H|^2 S_X(f')df'$, where k is a PAPR-related variable [11]. The MSE, $\sigma_e^2 = \langle |e|\rangle^2$, becomes

$$\sigma_e^2 = \int |HC - 1|^2 S_X(f)\, df + \frac{k\int |H|^2 S_X(f')df'}{12\left(2^{n_b}-1\right)^2 B_e}\int |C|^2 df \; + \int S_N(f) df, \tag{4}$$

where the first term on RHS is the residual ISI, the second (last) is the quantization noise filtered by C (channel noise). Ref. [11] suggests that the integral over f in the second term is a constant independent of H, i.e., $p_c \triangleq \int |C|^2 df$. Minimizing σ_e^2, i.e, $\partial\sigma_e^2/\partial H = 0$, and $\forall f$

$$\frac{\partial}{\partial H}[|HC - 1|^2 S_X + \lambda_1 p_c\, |H|^2] = 0, \tag{5}$$

where $\lambda_1 = \frac{k\, S_X}{12(2^{n_b}-1)^2 B_e}$. The last term of σ_e^2 in (4) disappears since S_N is independent of H. Thus, the optimal H becomes

$$H_{\sigma_e^2}(f) = \frac{C^*(f) S_X(f)}{|C(f)|^2 S_X(f) + \lambda_1 p_c}. \tag{6}$$

A contradiction comes: Eqn. (6) converges to ZF for negligible quantization (large $n_b, \lambda_1 \to 0$), which does not agree with the reality since using ZF in DPE results in high PAPRs, which requires substantial RMS reduction (small α_h) to avoid driver nonlinearity as previously discussed or in [4,7]. A power constraint is therefore required.

Frequency-partitioned DPE Optimization

We highlight our difference compared to [11]: the new objective function consists of the error variances due to ISI, quantization noise, additive noise, as well as our proposed RMS control (or filter energy or power constraint) weighted by

$$J = \int |HC - 1|^2 S_X(f)\, df + S_Q \int |C|^2 df + \int S_N(f) df + \lambda_2 [\int |H|^2\, df - p_e], \tag{7}$$

where $\int |H|^2\, df \le p_e$. The filter energy, p_e, is not necessarily unity, but depends on the actual Tx power without causing driver saturation. Generally, different frequency contents have different impacts on PAPR, meaning different weights to control each subband's RMS, i.e.

$$J = \int |HC - 1|^2 S_X(f)\, df + \sum_i \lambda_{2,i}\left[\int_{f_{i-1}}^{f_i} |H|^2 S_X(f)\, df - p_{e,i}\right]. \tag{8}$$

The quantization term, S_Q, is discarded here since sufficiently large RMS avoids quantization effect [5,6]. This work only considers a low $[f_0, f_1]$ and a high $[f_1, f_2]$ frequency bands, i.e., $f_0 = 0, f_1 = f_a, f_2 = (1+\alpha)B/2$, where f_a is the frequency where the high-frequency subband starts, B is the symbol rate and α is the root-raised cosine roll-off factor, since experience shows that enhancing higher frequency components lead to a higher PAPR which compulsorily reduces the RMS. The above objective integral is thus partitioned into a lower and an upper frequency regions, such that

$$J = \int_0^{f_a} |HC - 1|^2 S_X(f)\, df + \int_{f_a}^{\frac{(1+\alpha)B}{2}} |HC - 1|^2 S_X(f)\, df + \lambda_{2,2}\left[\int_{f_a}^{(1+\alpha)B/2} |H|^2 S_X(f)\, df - p_e\right]. \tag{9}$$

The low-frequency pre-emphasis is assumed to have negligible change on signal's RMS ($\lambda_{2,1} = 0$), implying a zero-forcing (ZF) equalizer for $|f| \le f_a$, while the high-frequency part requires an

RMS control. Solving (9), the overall one-sided DPE filter becomes, with $R_{dB} = -20\log_{10}\lambda_2$,

$$H_{\mathrm{RMS}}(f, f_a, R_{dB}) = \begin{cases} 1/C(f), & \forall |f| \le f_a \\ \frac{C^*(f) S_X(f)}{|C(f)|^2 S_X(f) + \lambda_2}, & \forall |f| > f_a \end{cases}. \qquad (10)$$

The above equation shares a similar form as (6) but with different physical meanings. Our formulation is more self-contained than those in . In this work, the RMS control covers only the excess BW region, and thus $f_a = (1-\alpha)B/2$.

Experimental Results

Fig. 2 shows the experimental setup using 92.31 GBaud dual-polarization (DP) 16-QAM signal with $\alpha = 0.1$, with, a fixed driver gain, a constant-gain optical amplifier (EDFA) at Tx and a constant-power EDFA at Rx. Standard DSP was used to recover the signal, including a 71-tap 2×2 complex-valued equalizer and carrier phase recovery. The n^th root method [7], $H = \frac{1}{|C(f)|^{\beta}}$, was used for comparison. For a fair comparison, we also took the n^th root of the proposed filter in (2), i.e.,$H = H_{\mathrm{RMS}}(f, f_a, R_{\mathrm{dB}})^{\beta}$, and expect that the highest operational AIR can be attained at $\beta = 1$ (full DPE), i.e., H becomes (2). Fig. 3 (a) compares the $H(f)$'s shapes among all methods. Both ZF and the optimized n^th root approach ($\beta = 0.7$) enhance substantially high frequencies within the excess BW region (vertical dashed lines), while our proposed method "penalizes" them. Fig. 3 (b) presents the $H(f)$'s shapes for different values of R_{dB}. A larger depth parameter R_{dB} enhances more high frequencies but also reduces more ISI. Our approach also fully compensates the in-band ripples [16].

In Fig. 4 (a), small β's means less amount of pre-emphasis, and Rx DSP enhances more noise, reducing the operational AIR. Large β's (more pre-emphasis) are preferred to avoid Rx noise enhancement, but RMS drops accordingly,

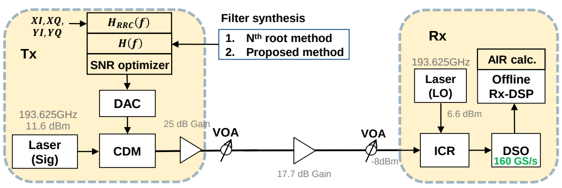

CDM: coherent driver modulator, ICR: integrated coherent receiver, DSO: digital sampling oscilloscope
VOA: variable optical attenuator, DAC: digital-to-analog converter, Sig: signal, LO: local oscillator

Fig. 2: Experimental setup; SNR optimizer from [5, 6].

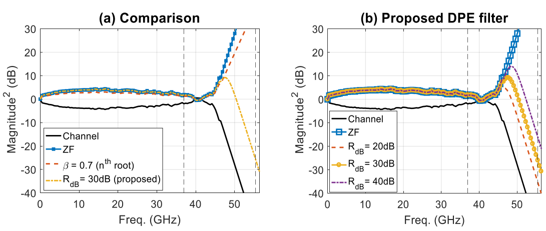

Fig. 3: a) DPE filter comparison between ZF, the optimized n^th root approach ($\boldsymbol{\beta = 0.7}$) and the proposed method. (b) The proposed $\boldsymbol{H_{\mathrm{RMS}}(f)}$ for different values of $\boldsymbol{R_{\mathrm{dB}}}$.

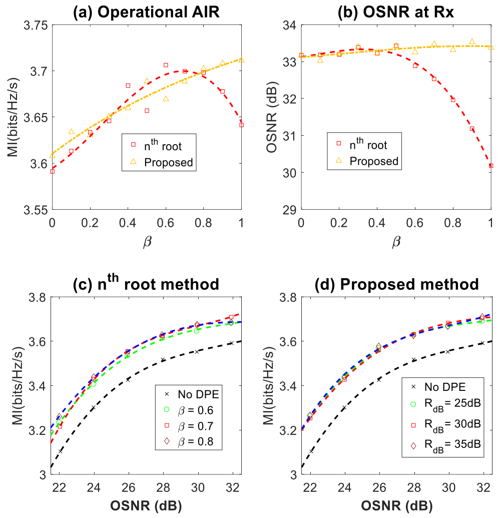

Fig. 4: (a) per-symbol mutual information (MI) and (b) OSNR at Rx (location A in Fig. 1). (c) Operational AIR versus OSNR for the n^th-root method and (d) for the proposed method for different parameter values.

revealed by Fig. 4 (b) (red) showing that the n^th root method with higher β's decreases OSNR at Rx. By controlling signal's RMS via shaping the high frequency components in (10), the OSNR can be restored (orange). Thus, our proposed method attains the best AIR at $\beta = 1$. Figs. 4 (c) and 4 (d) show the operational AIRs of the two methods versus OSNR. The n^th root method show obvious fluctuations when β changes, while the proposed method is insensitive to R_{dB}. Hence, the optimal R_{dB} can be pre-calculated once given a factory-calibrated Tx response for productization, and will not change much the performance due to aging or power reboot.

Conclusions

In this paper, we revisit the AIR due to the coupling between DPE and the BW-limited channel for short-reach applications. Generally, both input distribution and DPE should be optimized jointly to maximize the AIR, in practice.

We propose, for the first time, a self-contained DPE optimization theory with a RMS constraint (by the method of Lagrange multipliers): Given an input distribution, the high frequency signal components are shaped to avoid power loss, while the low-frequency part is fully compensated (a ZF for in-band ripples to avoid DSP penalty). The proposed method is parameter-insensitive, which can thus be pre-calculated given a factory-calibrated Tx S21 for productization. Other than ISI and RMS, more constraints, e.g., PAPR [15], peak power [8], etc. can be used for optimization. This, however, affects the DPE's robustness since more effort is required for parameter search, and the design becomes more sensitive to more parameters.

References

[1] E. Mao et al., “Where are the Boundaries Between IM-DD and Coherent?” in *Proceedings Optical Fiber Communication Conference*, Workshop S1F, 2023.
DOI: Not available.

[2] X. Zhou, C. F. Lam, R. Urata, and H. Liu , “State-of-the-Art 800G/1.6T Datacom Interconnects and Outlook for 3.2T, “ in *Proceedings Optical Fiber Communication Conference*, W3D.1, 2023.
DOI: Not available yet.

[3] D. Rafique, A. Napoli, S. Calabro and B.Spinnler., “Digital preemphasis in optical communication systems: On the DAC requirements for terabit transmission applications,” *Journal of Lightwave Technology*., vol. 32, no. 19, pp. 3247-3256, 2014.
DOI: 10.1109/JLT.2014.2343957.

[4] Z. Zhou, T. Odedeyi, B. Kelly, J. O'Carroll, R. Phelan, I. Darwazeh and Z. Liu., “Impact of Analog and Digital Pre-Emphasis on the Signal-to-Noise Ratio of Bandwidth-Limited Optical Transceivers,” *IEEE Photonics Journal*, vol. 12, no. 2, pp. 1-12, 2020.
DOI: 10.1109/JPHOT.2020.2966617.

[5] Y. Zhao, I, Fernandez de Jauregui Ruiz; A. Lorences-Riesgo, I.Demirtzioglou, S. Dris, Y. Frignac and G. Charlet, “A Novel Analytical Model of the Benefit of Partial Digital Pre-Emphasis in Coherent Optical Transponders,” in *Proceedings European Conference on Optical Communications*, pp. 1-4, 2020.
DOI: 10.1109/ECOC48923.2020.9333419.

[6] G. Böcherer, "Achievable Rates for Shaped Bit-Metric Decoding, “ arXiv:1410.8075. 2016.
DOI: 10.48550/arXiv.1410.8075.

[7] W. C. Ng, Q. Guo, J. Chang, T. Zhao, M. Qiu, X. Tang, Z. Jiang, and C. Li., “Low-Complexity RMS-enhanced Digital Pre-emphasis under Limited Transmitter Power and ENoB”, in *Proceedings Optical Fiber Communication Conference*, W2A.27, 2023.
DOI: Not available yet.

[8] Di Che and Xi Chen, “Does Probabilistic Constellation Shaping Benefit IM-DD Systems Without Optical Amplifiers?” *Journal of Lightwave Technology*, vol. 39, no. 15, pp. 4997–5007, 2021.
DOI: 10.1109/JLT.2021.3083530.

[9] B. M. Oliveira, J. H. Silva, M. S. Neves, F. P. Guiomar, M. C. R. Medeiros, and P. P. Monteiro, “Revisiting Probabilistic Constellation Shaping in Unamplified Coherent Optical Links”, in *Proceedings Optical Fiber Communication Conference*, Th3E.1, 2023.
DOI: Not available yet.

[10] J. Cho, L. Schmalen and P. J. Winzer, "Normalized Generalized Mutual Information as a Forward Error Correction Threshold for Probabilistically Shaped QAM," in *Proceedings European Conference on Optical Communications*, pp. 1-4, 2017.
DOI: 10.1109/ECOC.2017.8345872.

[11] A. Napoli, M. M. Mezghanni, T. Rahman, D. Rafique, R. Palmer, B. Spinnler, S. Calabro, C. Castro, M. Kuschnerov, and M. Bohn, “Digital Compensation of Bandwidth Limitations for High-Speed DACs and ADCs,” *Journal of Lightwave Technology,* vol. 34, no. 13, pp. 3053–3064, 2016.
DOI: 10.1109/JLT.2016.2535487.

[12] Leszek Szczecinski; Alex Alvarado, Bit-Interleaved Coded Modulation: Fundamentals, Analysis and Design, Wiley-IEEE Press, 2015.

[13] S. T. Le and J. Cho, “OSNR-Aware Digital Pre-Emphasis for High Baudrate Coherent Optical Transmissions,” in *Proceedings Optical Fiber Communication Conference*, M3H.4, 2022.
DOI: 10.1364/OFC.2022.M3H.4.

[14] Y. Mori, H. Hasegawa, and K. Sato, “Joint pre-, inline-, and post-compensation of spectrum narrowing caused by traversing multiple optical nodes,” in *Proceedings European Conference on Optical Communications*, P1.SC3.45, 2017.
DOI: 10.1109/ECOC.2017.8345928.

[15] Z. Qiang, Y. Hong, and H. Zhang, “Peak-to-average Power Ratio Constrained Digital Pre-emphasis for Short-reach Coherent Systems with Transmitter Bandwidth Limitation ,” in *Proceedings* Asia Communications and Photonics Conference, 2022.
DOI: 10.1109/ACP55869.2022.10088706.

[16] M. Sato, M. Arikawa, H. Noguchi, J. Matsui, J. ’i. Abe, and E. Le Taillandier de Gabory, “Inline Optical Compensation of Group Delay Ripple for Long-haul Transmission Using Offloaded 2×2 MIMO Filter”, in *Proceedings Optical Fiber Communication Conference*, W3E.6, 2023.
DOI: Not available yet.